Critical scaling analysis of the itinerant ferromagnet $Sr_{1-x}Ca_xRuO_3$

D. Fuchs,[1] M. Wissinger,[1] J. Schmalian,[1,2] C.-L. Huang,[1,3] R. Fromknecht,[1] R. Schneider,[1] and H. v. Löhneysen[1,3]

[1]*Institut für Festkörperphysik, Karlsruher Institut für Technologie, 76021 Karlsruhe, Germany*

[2]*Institut für Theorie der Kondensierten Materie, Karlsruher Institut für Technologie, 76128 Karlsruhe, Germany*

[3]*Physikalisches Institut, Karlsruher Institut für Technologie, 76128 Karlsruhe, Germany*

(Received 9 October 2013; revised manuscript received 28 March 2014; published 5 May 2014)

The critical behavior of $Sr_{1-x}Ca_xRuO_3$ was investigated by a scaling analysis based on the Arrott-Noakes equation of state. The critical exponents β, γ, and δ of the magnetic critical behavior were extracted for samples with $0 \leqslant x \leqslant 0.6$. The ferromagnetic system exhibits a smooth suppression of the Curie temperature T_C to zero at a critical concentration $x_c \approx 0.7$. The ordered magnetic moment decreases simultaneously as expected for itinerant ferromagnets, however, does not vanish completely at x_c, indicating small magnetic clusters or inhomogeneities. For $x = 0$, mean-field like exponents are observed. With increasing x, the critical exponents β, γ, and δ vary nearly linearly from $\beta \approx 0.5$, $\gamma \approx 1$, and $\delta \approx 3$ for $x = 0$ to $\beta \approx 1$, $\gamma \approx 0.9$, and $\delta \approx 1.6$ for $x \approx 0.6$. The Widom scaling relation is always met for $x \leqslant 0.6$. Despite the systematic evolution of the critical exponents as a function of x, the exponents cannot be described by any of the universality classes known for classical standard models. The particular trend of the effective critical exponents may be possibly explained by a strong-disorder line of fixed points; the vicinity to x_c suggests that this behavior is caused by the vicinity to a quantum phase transition.

DOI: 10.1103/PhysRevB.89.174405 PACS number(s): 75.40.−s, 75.50.−y, 75.47.Lx

I. INTRODUCTION

The suppression of itinerant ferromagnetism in the perovskite ruthenates $Sr_{1-x}Ca_xRuO_3$ (SCRO) with increasing Ca substitution has attracted significant interest. The evolution of the ground state from ferromagnetic to paramagnetic in the itinerant system around $x \approx 0.7$ has been related to a ferromagnetic quantum phase transition (QPT) [1]. In the vicinity of such a QPT, quantum critical fluctuations can yield new effects such as non-Fermi-liquid behavior as observed in many experiments [2,3]. However, the critical scaling of the order parameter near a ferromagnetic QPT has been investigated only rarely. Experimental as well as theoretical results suggest the nature of the ferromagnetic QPT as being discontinuous [4–7]. A profound understanding of the critical phenomena in the vicinity of a QPT is still challenging.

$SrRuO_3$ has an orthorhombic perovskite structure with a space group *Pbnm* [8]. The distortion from the ideal ABO_3 perovskite structure (*Pm*-3*m*) is generated by a tilting of the RuO_6 octahedra, which increases with increasing chemical substitution of Sr^{2+} by smaller Ca^{2+} ions. T_C decreases from about 160 K for $x = 0$ to zero for $x \approx 0.7$. Although the spin susceptibility indicates a negative Weiss temperature for $x > 0.7$, suggesting an antiferromagnetic ground state, it has been shown that $CaRuO_3$ is still metallic and at the verge of a ferromagnetic instability [8].

First-principles calculations by Mazin and Singh [9] describe the suppression of T_C in SCRO within the context of band-structure-based Stoner theory. The cooperative RuO_6 site rotation that bends the O-Ru-O bond angle from 163° in $SrRuO_3$ to 148° in $CaRuO_3$ reduces the band degeneracy and therefore the density of electronic states at the Fermi energy, $\rho(\varepsilon_F)$, so that the Stoner criterion for ferromagnetism is no longer met in $CaRuO_3$. The *A*-site size variation in the perovskite structure introduced by the smaller Ca^{2+} ion also affects the reduction of T_C [10] but has apparently little to do with the complete suppression of T_C in $CaRuO_3$. Since the susceptibility $\chi(T)$ of SCRO ($x > 0$) usually deviates from the Curie-Weiss law below T_C of $SrRuO_3$, Jin *et al.* [11] argued that the T_C reduction and final complete suppression likely appears to be correlated to the anomalous paramagnetic $\chi(T)$, typical for a diluted ferromagnetic system [12], for which Griffiths [13] predicted a nonanalytical susceptibility below T_C of the parent compound. The introduction of the more acidic Ca^{2+} ion and the reduction of the O-Ru-O bond angle weaken the interatomic spin-spin interaction. Thus, Jin *et al.* suggest that the suppression of T_C in SCRO is likely caused by the dilution of ferromagnetic spin-spin coupling along Ru-O-Ru bonds. Muon spin relaxation (μSR) measurements that have a unique sensitivity to minute volume fractions of magnetically ordered and paramagnetic regions also indicate magnetic phase separation around $x = 0.7$ [7]. Demkó *et al.* [14] likewise reported on a disorder-induced extension of the ferromagnetic phase, developing a pronounced tail over a broad range of the composition x and leading to a rounding of the QPT at x_c.

Generally, the transition of itinerant ferromagnets at finite temperature can be described quite well by mean-field or classical theories since the Ginzburg regime in itinerant systems is usually rather narrow. For example, specific-heat, resistivity, and magnetization data of $SrRuO_3$ scale with mean-field critical exponents, including Gaussian fluctuations [15]. In contrast, the critical behavior in the vicinity of a QPT is rather unclear. Systems where T_C is suppressed by chemical [16–18] or hydrostatic pressure [4,19] often follow mean-field scaling. However, deviations from classical critical exponents are more often observed in the case of chemical substitution [20,21]. In μSR measurements, the SR rate exhibits critical slowing down of spin fluctuations near T_C for ferromagnetic SCRO with $0 \leqslant x \leqslant 0.65$, consistent with the expected behavior for itinerant-electron ferromagnets. The disappearance of critical slowing down for $x = 0.7$ may indicate a first-order evolution of the ferromagnetic to paramagnetic transition triggered by quantum fluctuations [7,22].

To shed light on the critical behavior of SCRO when approaching the QPT, we have carried out a systematic study of

the magnetization as a function of the Ca concentration x. The critical exponents β, γ, and δ were determined by a detailed scaling analysis based on the Arrott-Noakes [29] equation of state, where the magnetic critical exponents are defined for the magnetization M, the magnetic field strength H, and the reduced temperature $\tau = (T - T_C)/T_C$ as follows: $M \propto \tau^{\beta}$ for $\tau < 0$, $M \propto H^{1/\delta}$ for $\tau = 0$, and $\chi \propto \tau^{-\gamma}$ for $\tau > 0$. For $x = 0$, typical mean-field like exponents, i.e., $\beta \approx 0.5$, $\gamma \approx 1$, and $\delta \approx 3$ are observed; however, β, γ, and δ change systematically with increasing x towards critical exponents $\beta \approx 1$, $\gamma \approx 0.9$, and $\delta \approx 1.6$ at $x \approx 0.7$. The Widom scaling relation, $\gamma/\beta = \delta - 1$, is always obeyed over the measured concentration range. However, the critical exponents cannot be explained by any of the universality classes of known classical standard models. Our results will be discussed with respect to a crossover from mean-field like behavior at $x = 0$ to a line of fixed points that might emerge in the strong disorder limit as the system approaches the QPT at or near x_c.

II. EXPERIMENTAL

Polycrystalline samples of SCRO were prepared by solid-state sintering using $SrCO_3$ (99.99%), $CaCO_3$ (99.99%), and RuO_2 (99.99%) as starting materials. Nominal compositions of the powders ($0 \leqslant x \leqslant 1$) were mixed, milled, and calcinated for 10 h at 900 °C. Then, the product was milled again, pressed to pellets, and sintered in a Pt crucible at 1370 °C for 30 h. The structural properties of the samples were characterized by powder x-ray diffraction at room temperature. Rietveld refinement of the diffraction spectra resulted in stoichiometric single-phase material with symmetry *Pbnm* (No. 62). With increasing Ca concentration, the orthorhombic distortion increases. The orthorhombic lattice parameters are displayed in Fig. 1(a). The data perfectly agree with values from literature [23,24].

To document the chemical composition and stoichiometry of the samples we carried out electron-dispersive x-ray spectroscopy (EDS) and wavelength-dispersive x-ray spectroscopy. The signal was integrated over an analyzed surface area of $50 \times 50\ \mu m^2$ and $1\ cm^2$, respectively. Both experiments result in a stoichiometric composition of the sample. Results of the EDS analysis are shown in Fig. 1(b). The samples are stoichiometric in accordance with the nominal composition indicated by solid lines in Fig. 1(b). However, the techniques used are not sensitive enough to detect possible phase separation effects on a microscopic length scale below some μm.

Magnetization measurements were carried out using a superconducting quantum interference device (SQUID) from Quantum Design in the temperature and magnetic field range of 5–300 K and 0–7 T, respectively. A first estimation of the Curie temperature, T_C^*, the Weiss temperature θ, and the paramagnetic effective moment m_{eff}, were deduced from the magnetic susceptibility $\chi = M/H$ at $\mu_0 H = 20$ mT. T_C^* was determined by the minimum of $d\chi/dT$, θ by the extrapolation of $1/\chi$ vs T above T_C to $1/\chi = 0$ and m_{eff} by the slope of $1/\chi$ vs T well above T_C^*. The saturated or maximum magnetic moment, m_{max}, was measured at $T = 5$ K and $\mu_0 H = 7$ T. The magnetic properties, i.e., T_C^* and θ vs the Ca concentration x, are shown in Fig. 1(c). The magnetic moments m_{eff} and m_{max} vs x are displayed in Fig. 1(d).

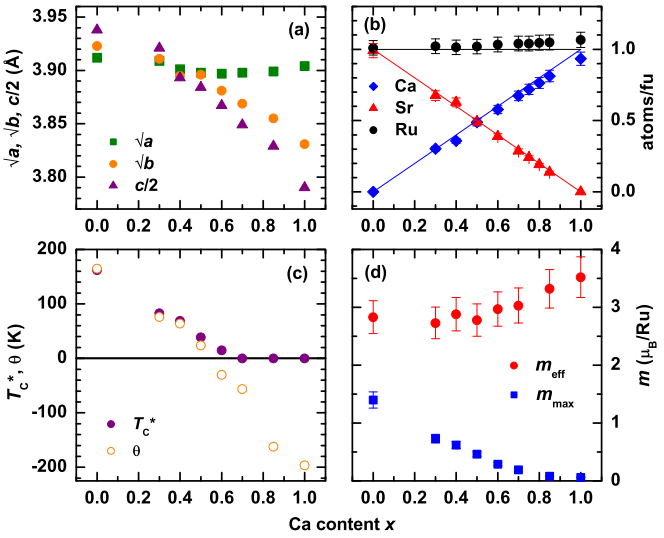

FIG. 1. (Color online) Structural and magnetic properties of the polycrystalline SCRO samples as a function of the Ca content x. (a) Orthorhombic lattice parameters determined at room temperature from Rietveld refinement; (b) chemical composition with respect to the Ca, Sr, and Ru content as determined by EDS analysis; (c) Curie temperature T_C^*, as determined by the minimum of $d\chi/dT$ and Weiss temperature θ; and (d) maximum magnetic moment m_{max} at $T = 5$ K and $\mu_0 H = 7$ T and effective magnetic moment m_{eff} determined by the slope of $1/\chi$ vs T.

The magnetic properties are consistent with data published in the literature [23,25]. T_C^* decreases with increasing x and vanishes at a critical concentration $x_c \approx 0.7$. Concomitantly, θ decreases likewise and becomes negative for $x > 0.5$. In the ferromagnetic region, m_{eff} is nearly constant and amounts to about 2.8 μ_B/Ru, which corresponds to the spin-only value of a localized electron model of a low-spin ($S = 1$) configuration of SCRO. This has been also observed by Okamoto *et al.* for $x < 0.7$ [26]. Above x_c, m_{eff} increases to 3.5 μ_B/Ru, which might indicate some additional contribution from orbital momentum. In contrast, the quasisaturated magnetic moment m_{max} decreases along with T_C, however, it does not disappear completely for $x = x_c$. Weak static magnetism for $x_c \leqslant x \leqslant 0.8$ has been also observed by μSR experiments and has been related to a phase separation between volumes with and without static magnetism [7]. Demkó *et al.* [14] likewise observed that the ferromagnetic phase is significantly extended by chemical disorder developing a pronounced tail over a broad range of composition x. The decrease of m_{max} with increasing x leads to a strong increase of the Rhodes-Wohlfarth ratio m_{eff}/m_{max} for $T_C \to 0$, as expected for the itinerant-electron model of ferromagnetism [27,28].

The critical scaling exponents of the magnetization, β, γ, and δ were extracted from a critical scaling approach based on the Arrott-Noakes equation of state [29]. Before starting with the presentation of our results, we briefly review the technique of data analysis. For the magnetization of a magnetic metal [30], the classical free energy of the Ginzburg-Landau-Wilson type is given by

$$F(M) = aHM + bM^2 + cM^4 + \ldots \qquad (1)$$

Minimizing the free energy, $\partial F/\partial M = 0$, leads to the mean field equation of state,

$$M^2 = a' + b'\frac{H}{M} + \ldots, \tag{2}$$

with $a' \propto 1/\chi$, being zero by definition at $T = T_C$. The plot of M^2 vs H/M is called the Arrott plot, leading to $M \propto H^{1/3}$ at T_C. A more general form of Eq. (2) that includes critical fluctuations and obeys the scaling laws near critical points was given by Arrott and Noakes [29]:

$$M^{1/\beta} = a* + b*\left(\frac{H}{M}\right)^{1/\gamma} + \ldots, \tag{3}$$

yielding the so-called modified Arrott plot with $M \propto H^{1/\delta}$ at T_C. This is the most general form of the equation of state near the critical point that respects the scaling laws of critical phenomena. The critical exponents β and γ can likewise be determined from scaling theory, which predicts the existence of a reduced equation of state of the form [31],

$$M/|T - T_C|^{\beta} = f_{\pm}(H/|T - T_C|^{\beta+\gamma}), \tag{4}$$

which results in two different curves, i.e., for the paramagnetic state (+) for $T > T_C$ and the ferromagnetic state (−) for $T < T_C$. The critical exponent δ can be deduced by using the Widom scaling relation [32] $\beta + \gamma = \beta\delta$.

The Arrott and Noakes relation is a direct consequence of the scaling behavior of the magnetization in the vicinity of a second-order phase transition:

$$M(t, H) = t^{\beta}\phi(H/t^{\beta\delta}), \tag{5}$$

where $t = (T_C - T)/T_C$. The function $\phi(x)$ is known in the limits of small and large arguments: $\phi(x \ll 1) \rightarrow$ const. and $\phi(x \gg 1) \propto x^{1/\delta}$. In our analysis, we have to take into account the fact that the samples are polycrystalline. In the extreme limit, where the magnetic easy axis varies on a characteristic length scale small compared to the magnetic correlation length, the random anisotropy would change the universality class of the transition, i.e., the values of the exponents. However, in our experiments, the typical size of the polycrystallites is some tens of microns, which is sufficiently large to obey the scaling relation [Eq. (5)] of a macroscopic system. Now, in each crystallite the exponents are of course those of a single-crystalline system. In each crystallite we have an effective field $H_{\text{eff}} = H \times f(\theta, \varphi)$ that depends on the orientation of the crystallites, characterized by the angles θ and φ. This leads to the magnetization density of the crystallite $M(\theta, \varphi)$. The measured magnetization density of the whole system is determined by the averaging over crystallites, with probability $p(\theta, \varphi)$ for a given orientation,

$$M = \int \sin\theta d\theta d\varphi p(\theta,\varphi) M(\theta,\varphi) = t^{\beta}\tilde{\phi}(H/t^{\beta\delta}), \tag{6}$$

where

$$\tilde{\phi}(x) = \int \sin\theta d\theta d\varphi p(\theta,\varphi)\phi(f(\theta,\varphi),x). \tag{7}$$

Thus, excluding pathological distribution functions, peaked sharply at angles perpendicular to the external field, averaging over crystallites yields the same scaling form, only with a modified scaling function. The behavior of the new scaling function is the same in the limits of small and large arguments, i.e., we will obtain the Arrott and Noakes relation, only with modified coefficients $a*$ and $b*$. This conclusion is supported by the experimental observation of same exponents in single crystalline and polycrystalline samples [33].

III. RESULTS AND DISCUSSION

To determine the critical exponents of the magnetic critical behavior of SCRO by a scaling approach based on the Arrott-Noakes equation of state, magnetic isotherms were recorded in evenly spaced temperature steps in the temperature range $0.97\ T_C \leqslant T \leqslant 1.03\ T_C$, where here T_C corresponds to the Curie temperature determined from the modified Arrott plots. From these plots, i.e., linearized plots of $M^{1/\beta}$ vs $(H/M)^{1/\gamma}$, the critical exponents β and γ, i.e., the fit parameters for linearization, as well as T_C, i.e., the isotherm through the origin, and the ordered magnetic moment, i.e., $M(H = 0)$ for $T < T_C$ are obtained. While our analysis was performed for polycrystalline samples, with varying orientation of the easy direction with respect to the applied magnetic field, the Arrott-Noakes equation of state is still valid for each crystallite. Averaging over the samples will affect the values of the coefficients $a*$ and $b*$ in Eq. (3) but will not affect the values of the critical exponents on T_C, as outlined above.

Figure 2 displays a subset of magnetization curves for $x = 0$, 0.3, 0.4, 0.5, and 0.6. Only six isotherms in the temperature range $0.97\ T_C \leqslant T \leqslant 1.03\ T_C$ are shown. For constant x and $\mu_0 H$, the magnetization decreases with increasing T. With increasing x, $m_{\max}(T \approx T_C)$ decreases. In Fig. 3, we display the modified Arrott plots for $x = 0$, 0.3, 0.4, 0.5, and 0.6. The same isotherms $M(H)$, as shown in Fig. 2, are displayed. The isotherm at $T = T_C$ yields the critical exponent δ, which is given by $M \propto H^{1/\delta}$. In addition, the critical exponents β and δ were determined by Arrott-Noakes scaling plots, where the scaled magnetization $M/|T - T_C|^{\beta}$ is plotted vs the scaled magnetic field $\mu_0 H/|T - T_C|^{\beta\delta}$. Within the critical temperature range, the correct δ leads to a collapse of the $M(H)$ data onto one branch for $T > T_C$ and one for $T < T_C$. The branches for $T > T_C$ and $T < T_C$ each collapse onto one curve. Figure 4 displays the scaling plots for the magnetization curves shown in Figs. 2 and 3. The scaling behavior is evident and demonstrates the consistency between modified Arrott plot and Arrott-Noakes scaling analysis. Nevertheless, the scaling is not always perfect, in particular for $x = 0$. However, since we were able to deduce the correct exponents for the peculiar case of $x = 0$, we conclude that the scaling is adequate for the more converging plots of the other samples.

The results of the scaling analysis are summarized in Fig. 5. Figure 5(a) displays T_C as deduced from the modified Arrott plots shown in Fig. 3 as well as the magnetic moment $m_{\max}$ at $T = 5$ K and $\mu_0 H = 7$ T vs x. T_C and $m_{\max}$ decrease roughly linearly with increasing x, where the relative decrease is nearly the same for both quantities. A linear extrapolation of T_C to zero yields the critical concentration $x_c \approx 0.7$, consistent with literature. However, $m_{\max}$ does not vanish completely at x_c, in line with the smearing of the quantum critical point proposed for strongly disordered metallic systems [34].

In Fig. 5(b), we show the evolution of the critical exponents β, γ, and δ as a function of Ca concentration x. The

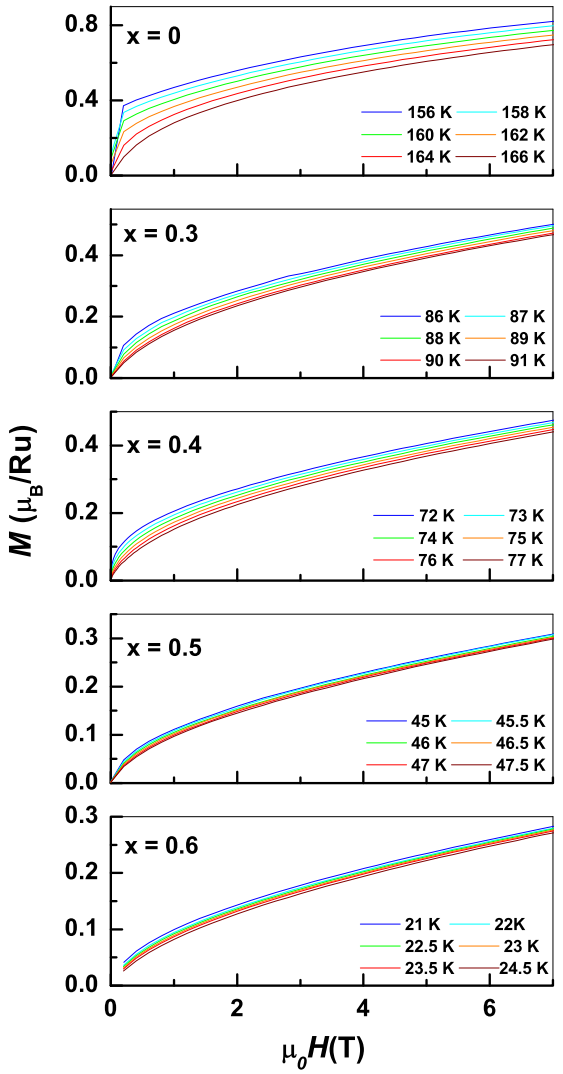

FIG. 2. (Color online) Magnetization curves M vs H of $Sr_{1-x}Ca_xRuO_3$ for $x = 0$, 0.3, 0.4, 0.5, and 0.6. Only six of the measured isotherms in the temperature range $0.97\ T_C \leqslant T \leqslant 1.03\ T_C$ are displayed. The magnetization decreases with increasing temperature. With increasing Ca concentration x, T_C as well as the magnetic moment around T_C at $\mu_0 H = 7$ T are found to decrease.

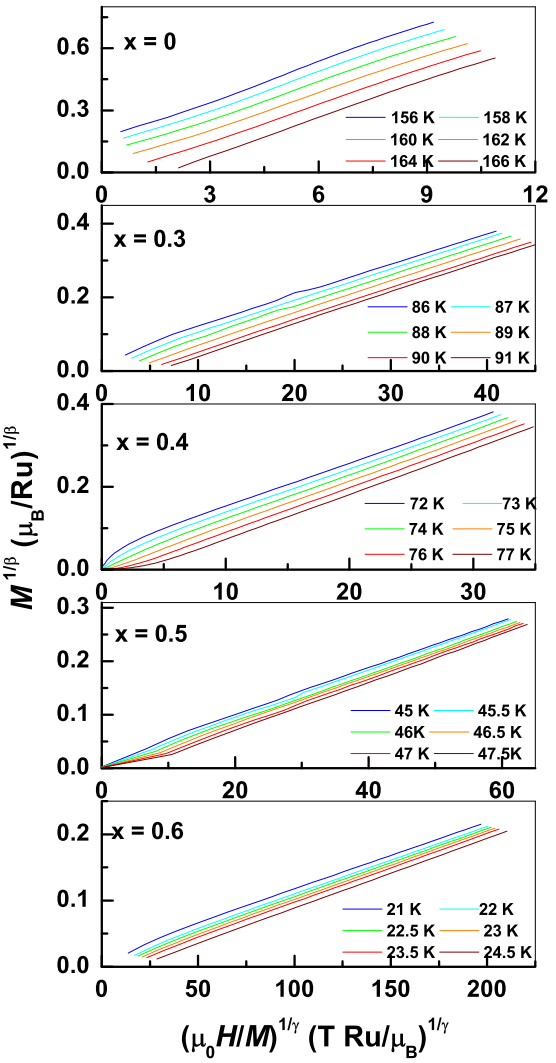

FIG. 3. (Color online) Modified Arrott plots of $Sr_{1-x}Ca_xRuO_3$ for $x = 0$, 0.3, 0.4, 0.5, and 0.6. The magnetization decreases with increasing temperature. $M(H)$ data are linearized by the fitting parameters β and γ in order to obtain the critical exponents (see text). The plots are shown for the same data as displayed in Fig. 2.

linearization of $M^{1/\beta}$ vs $(H/M)^{1/\gamma}$ shows some insensitivity to the choice of β and γ, which results in a non-negligible error. Within the experimental resolution, we were not able to deduce critical exponents for $x \approx 0.7$. Literature values from Kim *et al.* [15] and Itoh *et al.* [21] are included for comparison. For $x = 0$, mean-field like exponents, i.e., $\beta \approx 0.5$, $\gamma \approx 1$, and $\delta \approx 3$ are observed, which are in good agreement with the critical exponents found for $SrRuO_3$ single crystals by Kim *et al.* [15]. However, with increasing x, the critical exponents deviate systematically from the mean-field values showing unusual critical exponents and approaching $\beta \approx 1$, $\gamma \approx 0.9$, and $\delta \approx 1.6$ at $x \approx 0.6$. In a recent study, Cheng *et al.* [35] also have found a systematically growing convex curvature of the M^2 vs H/M isotherms with x for $x > 0$, indicating a steady increase of β above the mean-field value of 0.5. The authors have suggested local structural distortions as a source of the convex curvature. Itoh *et al.* [21] were able to extract a critical exponent of $\delta = 1.5$ for $x = 0.7$, which again is in perfect line with our results. In addition, the Widom relation, which relates the critical exponents to each other [32], i.e., $\gamma/\beta = \delta - 1$, is obeyed over the complete range of investigated x, which demonstrates the consistency and validity of the scaling analysis alike.

Despite the observed steady evolution of β, γ, and δ, the critical exponents cannot be explained by currently available theoretical models, nor by a universality class for known classical standard models [36]. Usually, if the critical dimension is reduced so that critical fluctuations become important, an opposite change of the mean-field critical exponents is expected, i.e., δ and γ should rather increase and β decreases. Also, proposals for effective exponents that govern the intermediate crossover regime between clean and disordered fixed points [37] have trends opposite to our findings.

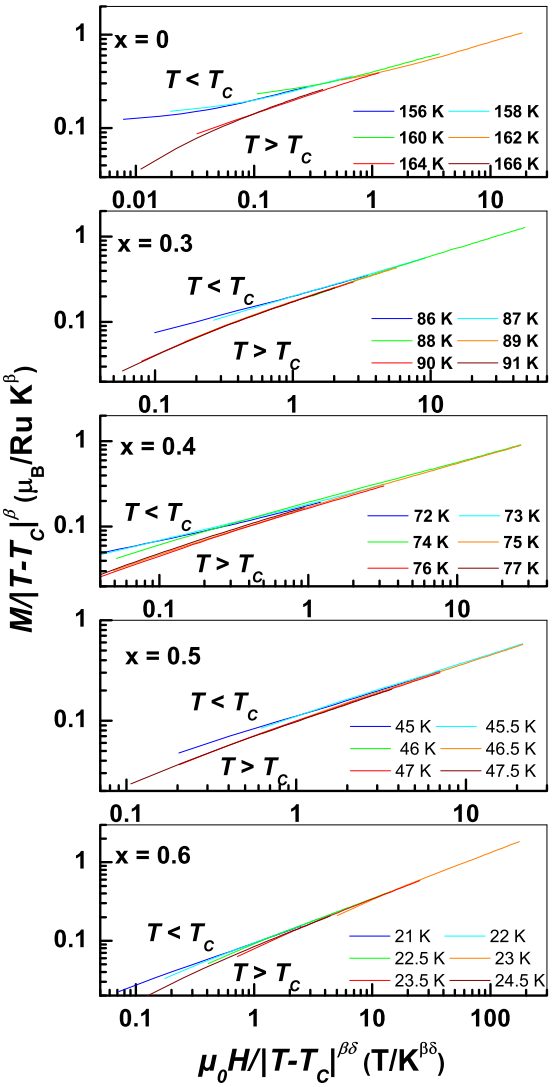

FIG. 4. (Color online) Arrott-Noakes scaling plots of $Sr_{1-x}Ca_xRuO_3$ for $x = 0$, 0.3, 0.4, 0.5, and 0.6. The $M(H)$ data curves collapse onto one branch each for $T < T_C$ and $T > T_C$. The two branches for $T < T_C$ and $T > T_C$ collapse onto one curve. The scaling plots are shown for the same data as displayed in Fig. 2.

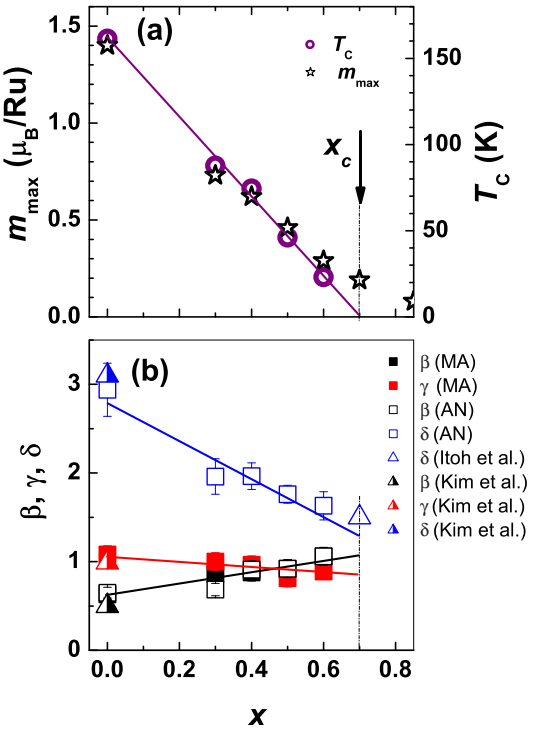

FIG. 5. (Color online) (a) T_C as deduced from modified Arrott plots (right-hand scale) and the magnetic moment m_{max} at $T = 5$ K and $\mu_0 H = 7$ T vs x (left-hand scale). The relative change of T_C and m_{max} with increasing x are nearly the same. A linear extrapolation of T_C to zero (solid line) yields the critical concentration $x_c \approx 0.7$. (b) Critical exponents β, γ, and δ as deduced from the modified Arrott (MA) plots and the Arrott-Noakes (AN) scaling plots as a function of the Ca concentration x error bars are indicated. Literature values from Kim *et al.* [15] and Itoh *et al.* [21] are included for comparison. The lines are guide to the eye indicating the nearly linear behavior of β, γ, and δ vs x.

Deviations from mean-field behavior occur when the reduced temperature τ is smaller than the reduced Ginzburg temperature $\tau_G = (1/32\pi^2)(k_B/2\Delta C_V \xi_0^3)^2$, where k_B is the Boltzmann constant, ΔC_V the jump of the specific heat at the phase transition, and ξ_0 the coherence length [38]. For $\tau < \tau_G$ critical fluctuations appear and are becoming important, where a proper prediction of the critical exponents is only valid in the temperature range $\tau < \tau_G$, known as the Ginzburg criterion. Mean-field behavior was observed for $SrRuO_3$ by Kim *et al.* very close to T_C for $\tau = 0.0003$, i.e., $\Delta T \approx 50$ mK, from which the authors deduced a correlation length $\xi_0 > 7$ Å. Because of the metallic behavior of $Sr_{1-x}Ca_xRuO_3$, it is not expected that ξ_0 shrinks with increasing x. In contrast, ΔC_V clearly decreases with increasing x [39], which possibly leads to an increase of τ_G, making it in principle less difficult to measure critical behavior. Nevertheless, the measured exponents should be regarded rather as effective critical exponents.

A continuous shift of mean-field critical exponents to lower values of δ and γ with increasing chemical substitution towards $T_C = 0$ has been previously observed by Butch and Maple for the itinerant ferromagnet $URu_{2-x}Re_xSi_2$ [40]. Since γ and $(\delta - 1)$ are decreasing to zero for $T_C \to 0$, a crossover to a first-order transition at the quantum critical point has been discussed by these authors [40]. Itinerant ferromagnets, i.e., $ZrZn_2$, UGe_2, and MnSi, indeed show a generic phase diagram, where the nature of the ferromagnetic transition changes from second order to first order at a tricritical point and surfaces of first-order transitions terminating in quantum critical end points emerge [41]. However, although γ and $(\delta - 1)$ are decreasing for SCRO as well, the values clearly do not tend to zero at x_c, thus excluding any crossover to a first-order transition.

From the frequency dependence of the susceptibility (not shown), dynamical critical scaling for $x = 0.6$ leads to a dynamical exponent $z\nu \approx 7.7$, where z is the dynamical critical exponent and ν the critical exponent of the spin correlation length. The exponent agrees nearly perfectly with the value expected for spin glasses [42], attesting magnetic inhomogeneities, as already indicated in Fig. 5(a) by the presence of a small magnetic moment for $x \geqslant 0.7$ also

observed by other groups [14,20]. Disorder may likewise lead to new critical exponents if the specific-heat exponent $\alpha > 0$, known as the Harris criterion [43]. For SCRO, the structural distortion, caused by the chemical substitution of Ca for Sr, may indeed lead to magnetocrystalline anisotropy and thus to $3d$ Ising-like behavior, d being the spatial dimensionality for which $\alpha > 0$. However, a field-theoretical approach of the pure-Ising-to-random crossover yields a steady increase of γ [37], which contrasts experimental trend.

In the following, we want to discuss the evolution of the classical critical exponents towards $x = x_c$, where the transition temperature vanishes. At first glance it might be tempting to explain the new critical exponents observed here in terms of quantum critical fluctuations that occur in the vicinity of x_c. Indeed, for the case $d = 3$, Belitz and Kirkpatrick deduced quantum critical exponents of $\delta = 3/2$, $\beta = 2$, and $\gamma = \beta(\delta - 1) = 1$ [44], which deviate significantly from values of classical critical exponents. The new exponents are caused by soft or massless modes coupling to the order-parameter fluctuations and modifying the critical behavior. The extrapolation to $x = x_c$ of the quasiclassical critical exponents δ, which we deduced from our magnetization measurements at $T = T_C > 0$ [see Fig. 5(b)], indeed compares nearly perfectly with the predicted quantum critical exponent. However, these quantum critical exponents refer to a $T = 0$ quantum critical point, while our measured exponents refer to a finite-temperature classical fixed point. For example, the exponent β of Ref. [44] measures the magnetization at zero temperature as function of $x - x_c$, i.e., $M(T = 0,\ x) \propto (x - x_c)^{\beta}$, while our experiments measure $M(T,\ x_c) \propto (T - T_C)^{\beta}$, i.e., comparing both experiments is not sensible. Nevertheless, the vicinity to a quantum critical point seems to be important for the observed variations of the exponents. Quantum fluctuations can indeed lead to significant renormalizations of the low-energy theory that underlies the classical critical point. It is therefore possible that such quantum fluctuations enhance the role of disorder and drive the system into a new strong-coupling regime that is not easily accessible via the established perturbative coupling renormalization-group calculations. The continuous variation of the exponents then suggests that the system is governed by a line of fixed points, similar to the well-known Kosterlitz-Thouless theory of *XY* degrees of freedom in two dimensions.

IV. SUMMARY

In summary, the evolution of the critical behavior of $Sr_{1-x}Ca_xRuO_3$ was investigated as a function of the Ca substitution x. Critical exponents of the magnetization were extracted by a scaling analysis based on the Arrott-Noakes equation of state. For $x = 0$, mean-field like exponents are observed. The ferromagnetic system exhibits a smooth suppression of T_C with increasing x. T_C vanishes at a critical concentration $x_c \approx 0.7$. The ordered magnetic moment decreases alike, as expected for itinerant ferromagnets, however, it does not vanish at x_c. The residual magnetic moment at and even beyond x_c may be explained by small magnetic clusters or inhomogeneities, which is supported by the dynamical scaling of the susceptibility. With increasing x, the critical exponents β, γ, and δ change nearly linearly from $\beta \approx 0.5$, $\gamma \approx 1$, and $\delta \approx 3$ for $x = 0$ to $\beta \approx 1$, $\gamma \approx 0.9$, and $\delta \approx 1.6$ for $x \approx 0.6$. The particular trend of the critical exponents may be due to a crossover from mean-field like behavior at $x = 0$ to a nontrivial strong-coupling and strong-disorder line of fixed points boosted by the vicinity to the QPT at $x = x_c$.

ACKNOWLEDGMENTS

Part of this work was supported by the German Science Foundation (DFG) in the framework of the DFG Research Unit 960 "Quantum Phase Transitions". D.F. is grateful to Roland Hott for providing useful software tools for data analysis.

[1] K. Yoshimura, T. Imai, T. Kiyama, K. R. Thurber, A. W. Hunt, and K. Kosuge, Phys. Rev. Lett. **83**, 4397 (1999).
[2] M. B. Maple, M. C. de Andrade, J. Herrmann, Y. Dalichaouch, D. A. Gajewski, C. L. Seaman, R. Chau, R. Movshovich, M. C. Aronson, and R. Osborn, Low Temp. Phys. **99**, 223 (1995).
[3] H. v. Löhneysen, A. Rosch, M. Voijta, and P. Wölfle, Rev. Mod. Phys. **79**, 1015 (2007).
[4] M. Uhlarz, C. Pfleiderer, and S. M. Hayden, Phys. Rev. Lett. **93**, 256404 (2004).
[5] C. Pfleiderer and A. D. Huxley, Phys. Rev. Lett. **89**, 147005 (2002).
[6] A. V. Chubukov, C. Pépin, and J. Rech, Phys. Rev. Lett. **92**, 147003 (2004).
[7] Y. J. Uemura, T. Goto, I. M. Gat-Malureanu, J. P. Carlo, P. l. Russo, A. T. Savici, A. Aczel, G. J. McDougall, J. A. Rodriguez, G. M. Luke, S. R. Dunsiger, A. McCollam, J. Arai, Ch. Pfleiderer, P. Böni, K. Yoshimura, E. Baggio-Saitovich, M. B. Fontes, J. Larrea, Y. V. Sushko, and J. Sereni, Nat. Phys. **3**, 29 (2007).
[8] J. M. Longo, P. M. Raccah, and J. B. Goodenough, J. Appl. Phys. **39**, 1327 (1968).
[9] I. I. Mazin and D. J. Singh, Phys. Rev. B **56**, 2556 (1997).
[10] J. P. Attfield, Cryst. Eng. **5**, 427 (2002).
[11] C. Q. Jin, J. S. Zhou, J. B. Goodenough, Q. Q. Liu, J. G. Zhao, L. X. Yang, Y. Yu, R. C. Yu, T. Katsura, A. Shatskiy, and E. Ito, Proc. Natl. Acad. Sci. USA **105**, 7115 (2008).
[12] A. J. Bray, Phys. Rev. Lett. **59**, 586 (1987).
[13] R. B. Griffiths, Phys. Rev. Lett. **23**, 17 (1969).
[14] L. Demkó, S. Bordács, T. Vojta, D. Nozadze, F. Hrahsheh, C. Svoboda, B. Dóra, H. Yamada, M. Kawasaki, Y. Tokura, and I. Kézsmárki, Phys. Rev. Lett. **108**, 185701 (2012).
[15] D. Kim, B. L. Zink, F. Hellman, S. McCall, G. Cao, and J. E. Crow, Phys. Rev. B **67**, 100406(R) (2003).
[16] K. Yoshimura and Y. Nakamura, Solid State Commun. **56**, 767 (1985).
[17] D. A. Sokolov, M. C. Aronson, W. Gannon, and Z. Fisk, Phys. Rev. Lett. **96**, 116404 (2006).
[18] N. T. Huy, A. Gasparini, D. E. de Nijs, Y. Huang, J. C. P. Klaasse, T. Gortenmulder, A. de Visser, A. Hamann, T. Görlach, and H. v. Löhneysen, Phys. Rev. Lett. **99**, 067006 (2007).

[19] T. Akazawa, H. Hidakau, H. Kotegawa, T. C. Kobayashi, T. Fujiwara, E. Yamamoto, Y. Haga, R. Settai, and Y. Onuki, J. Phys. Soc. Jpn. **73**, 3129 (2004).
[20] S. Ubaid-Kassis, T. Vojta, and A. Schroeder, Phys. Rev. Lett. **104**, 066402 (2010).
[21] Y. Itoh, T. Mizoguchi, and K. Yoshimura, J. Phys. Soc. Jpn. **77**, 123702 (2008).
[22] I. M. Gat-Malureanu, J. P. Carlo, T. Goko, A. Fukaya, T. Ito, P. P. Kyriakou, M. I. Larkin, G. M. Luke, P. L. Russo, A. T. Savici, C. R. Wiebe, K. Yoshimura, and Y. J. Uemura, Phys. Rev. B **84**, 224415 (2011).
[23] F. Fukunaga and N. Tsuda, J. Phys. Soc. Jpn. **63**, 3798 (1994).
[24] H. Kobayashi, M. Nagata, R. Kanno, and Y. Kawamoto, Mater. Res. Bull. **29**, 1271 (1994).
[25] G. Cao, S. McCall, M. Shepard, J. E. Crow, and R. P. Guertin, Phys. Rev. B **56**, 321 (1997).
[26] J. Okamoto, T. Okane, Y. Saitoh, K. Terai, S. I. Fujimori, Y. Muramatsu, K. Yoshii, K. Mamiya, T. Koide, A. Fujimori, Z. Fang, Y. Takeda, and M. Takano, Phys. Rev. B **76**, 184441 (2007).
[27] P. Rhodes and E. P. Wohlfarth, Proc. Roy. Soc. A **273**, 247 (1963).
[28] E. P. Wolfarth, J. Magn. Magn. Mater. **7**, 113 (1987).
[29] A. Arrott and J. E. Noakes, Phys. Rev. Lett **19**, 786 (1967).
[30] A. Arrott, Phys. Rev. **108**, 1394 (1957).
[31] S. N. Kaul, J. Magn. Magn. Mater. **53**, 5 (1985).
[32] A. Hankey and H. E. Stanley, Phys. Rev. B **6**, 3515 (1972).
[33] Critical exponents deduced here from polycrystalline materials compare perfectly with those extracted from single crystal samples published in Refs. [15] and [21].
[34] T. Vojta, Phys. Rev. Lett. **90**, 107202 (2003).
[35] J. G. Cheng, J. S. Zhou, J. B. Goodenough, and C. Q. Jin, Phys. Rev. B **85**, 184430 (2012).
[36] M. F. Collins, *Magnetic Critical Scattering* (Oxford University Press, Oxford Series on Neutron Scattering in Condensed Matter, Vol. 4, 1989).
[37] P. Calabrese, P. Parruccini, A. Pelissetto, and E. Vicari, Phys. Rev. E **69**, 036120 (2004).
[38] V. L. Ginzburg, Sov. Phys. Solid State **2**, 1824 (1961).
[39] T. Kiyama, K. Yoshimura, K. Kosuge, H. Michor, and G. Hilscher, J. Phys. Soc. Jpn. **67**, 307 (1998).
[40] N. P. Butch and M. B. Maple, Phys. Rev. Lett. **103**, 076404 (2009).
[41] D. Belitz, T. R. Kirkpatrick, and J. Rollbühler, Phys. Rev. Lett. **94**, 247205 (2005).
[42] A. T. Ogielski, Phys. Rev. B **32**, 7384 (1985).
[43] A. B. Harris, J. Phys. C: Solid State Phys. **7**, 1671 (1974).
[44] D. Belitz, T. R. Kirkpatrick, M. T. Mercaldo, and S. L. Sessions, Phys. Rev. B **63**, 174428 (2001).